

# OBSERVATION OF ELECTRON-ION EFFECTS AT RHIC TRANSITION\*

J. Wei<sup>†</sup>, U. Iriso, M. Bai, M. Blaskiewicz, P. Cameron, R. Connolly, A. Della Penna, W. Fischer, H. Huang, R. Lee, R. Michnoff, V. Ptitsyn, T. Roser, T. Satogata, S. Tepikian, L. Wang, S.Y. Zhang  
Brookhaven National Laboratory, New York, USA

## Abstract

Electron cloud is found to be a serious obstacle on the upgrade path of the Relativistic Heavy Ion Collider (RHIC). At twice the design number of bunches, electron-ion interactions cause significant instability, emittance growth, and beam loss along with vacuum pressure rises when the beam is accelerated across the transition.

## INTRODUCTION

Electron cloud effects previously observed in RHIC mainly include vacuum pressure rise, experimental background rise, and instrumentation interferences [1]-[4]. Beam-induced electron multipacting is expected to be the leading mechanism producing the cloud (Fig. 1).

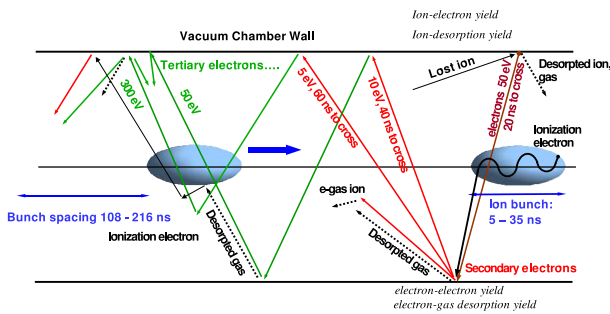


Figure 1: Electron build-up at RHIC shown as a result of beam-induced electron multipacting.

Table 1: RHIC parameters during year 2005 *e*-I study.

Ring revolution period	12.79	$\mu$ s
Aperture, IR (2/6/8/10, 4/12)	7, 12	cm
Aperture (arc, triplet)	7, 13	cm
Beam species	Cu <sup>29+</sup>	
Energy, injection - top	9.8 - 100	GeV/u
Transition energy, $\gamma_T$	22.9	
Bunch intensity	$5 \times 10^9$	
Bunch center spacing	108	ns
Bunch length at transition, full	$\sim 5$	ns
Electron bounce frequency	$\sim 400$	MHz
Peak bunch potential	$\sim 1.6$	kV
<i>e</i> <sup>-</sup> energy gain upon acceleration	$\sim 300$	V

Due to the slow ramp-rate of the superconducting magnets, the ion beams in RHIC often suffer emittance growth and beam loss upon transition ( $\gamma_T$ ) crossing. Near  $\gamma_T$ , most of the undesired effects (chromatic nonlinearity, self-field mismatch, and impedance-induced instabilities) on a nominal beam of 216 ns bunch spacing are mitigated by the  $\gamma_T$ -

\* Work performed under the auspices of the US Department of Energy.

<sup>†</sup> jwei@bnl.gov

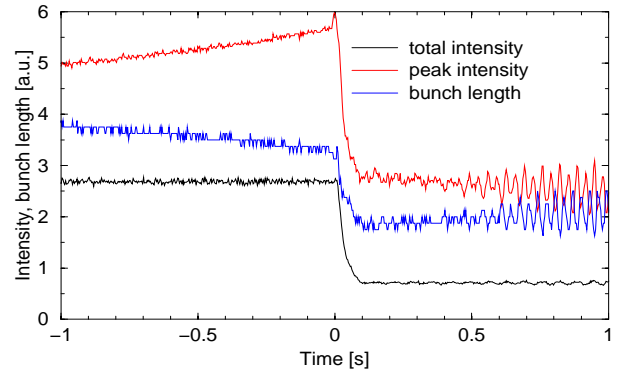


Figure 2: Beam loss and bunch size variation of bunch #40 at transition with  $V_{rf} = 300$  kV and  $b_{oct} = -3$  unit.

jump scheme, pulsing the quadrupole correctors to vary  $\gamma_T$  by about 1 unit during 30 ms around  $\gamma_T$  [5, 6].

Dedicated studies are performed in 2005 with Cu bunches of half the nominal spacing (108 ns) crossing  $\gamma_T$  (Table 1). For simplicity, only one of the two rings (blue) is populated with 40 bunches in 1/3 of the circumference. In addition to the *e*-cloud effects (pressure rise, electron flux) occurring during a time of seconds as the beam approaches  $\gamma_T$  (Fig. 2), strong electron-ion (*e*-I) interactions (instabilities, emittance growth, beam loss) are observed during a time of tens of ms after transition when the ion motion is non-adiabatic.

## OBSERVATIONS

This section lists *e*-cloud observations of year 2005.

### Beam loss

With the harmonic 360 RF system at 200 kV voltage ( $V_{rf}$ ), beam losses are measured with the wall current monitor (WCM) across  $\gamma_T$  varying from 13% for the first to

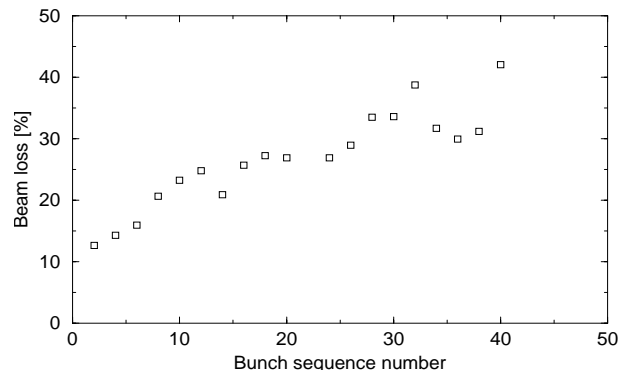


Figure 3: Beam loss at transition as a function of bunch sequence number with  $V_{rf}=200$  kV and  $b_{oct} = -3$  unit.

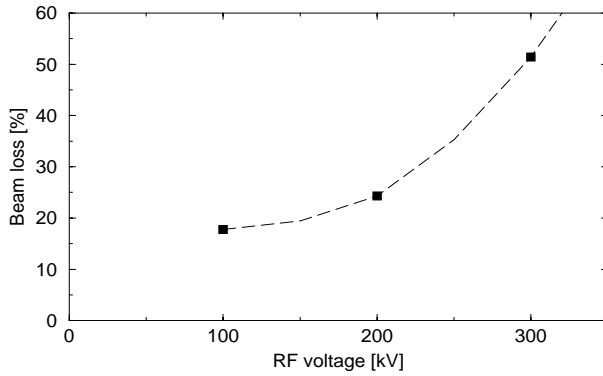


Figure 4: Average beam loss at transition as a function of the RF voltage with  $b_{oct} = -3$  unit.

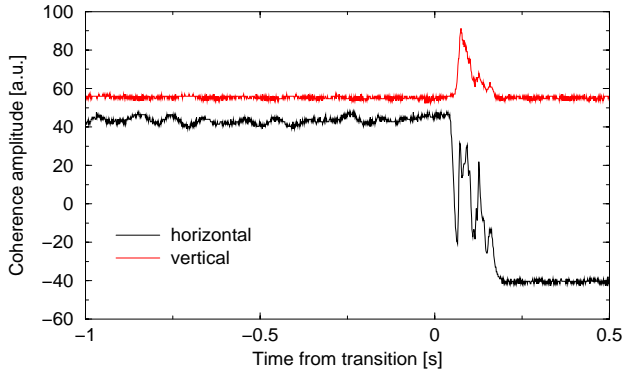


Figure 5: Coherence signal of bunch #40 from the turn-by-turn BPM data. The horizontal instability signal is within a step caused by the orbit shift due to  $\gamma_T$ -jump.

42% for the last bunch (Fig. 3). In comparison, at the nominal 216 ns spacing the loss is less than 5% uniform across the bunch train. The loss increases significantly with the RF voltage as the peak beam intensity, electron energy gain, and  $e$ -multipacting all increase (Fig. 4). Fig. 2 shows about 73% loss of bunch #40 within 0.1 s after  $\gamma_T$ .

### Transverse fast instability

Fig. 5 shows the transverse coherence signal defined as the transverse centroid displacement measured from the turn-by-turn beam position monitor (BPM). A transverse instability occurs immediately after transition for about 0.1 s, leading to beam loss and emittance growth that are increasingly severe for later bunches of the bunch train. Fig. 6 shows the mean square of difference signal measured by a “button” BPM at 0.5 ns sampling rate. Again, the horizontal signal is complicated by the  $\gamma_T$ -jump induced orbit shift. Both the instability and the beam loss are reduced by the damping effect of the octupole families (Fig. 7).

### Transverse emittance growth

Bunch-train dependent transverse emittance growth at  $\gamma_T$  is observed when the beam loss is moderate (Fig. 8). With a larger beam loss (e.g.,  $V_{rf} \geq 200$  kV cases), the dependence becomes not obvious, presumably because particles of larger emittance are lost. An accurate measurement is difficult with the ionization profile monitor when

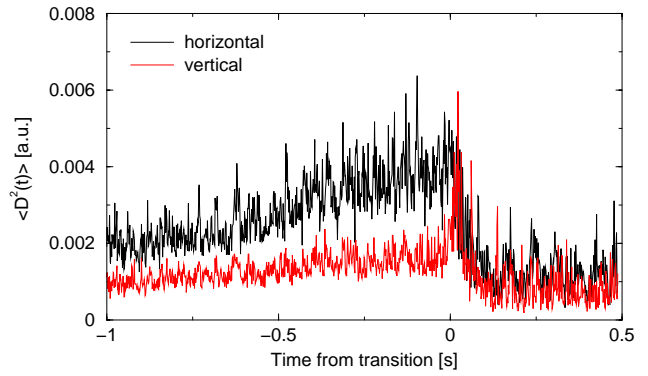


Figure 6: Mean square of the difference displacement measured by the “button” BPM sampling every 0.5 ns.

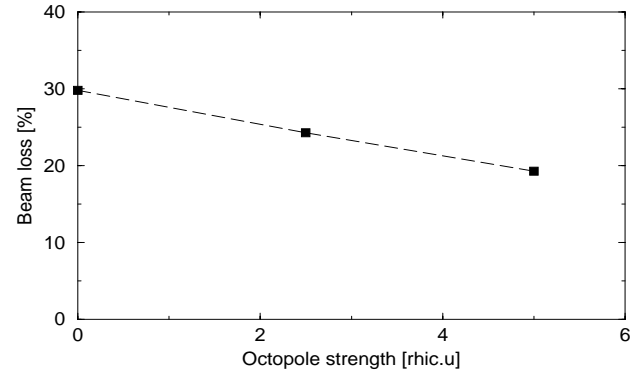


Figure 7: Average beam loss at transition as a function of the octupole magnet strength  $|b_{oct}|$  with  $V_{rf} = 200$  kV.

the loss-related pressure rise is excessive.

### Longitudinal profile variation

Fig. 9 shows that the beam loss occurs mostly at the trailing edge of the bunch matching the  $e$ -cloud mechanism. In the longitudinal direction, neither instability nor bunch-train dependent emittance growth are observed.

### Electron flux and vacuum pressure rise

Fig. 10 shows the electron flux on the wall measured by a retarding-field electron detector [2]. The flux increases

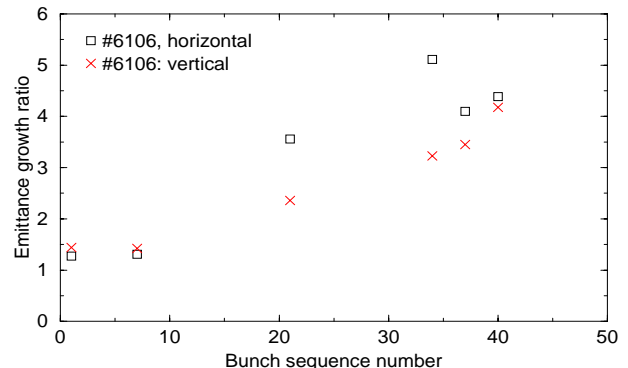


Figure 8: Bunch train dependence of the beam emittance growths at  $\gamma_T$  with  $V_{rf}=100$  kV and  $b_{oct} = -4$  unit.

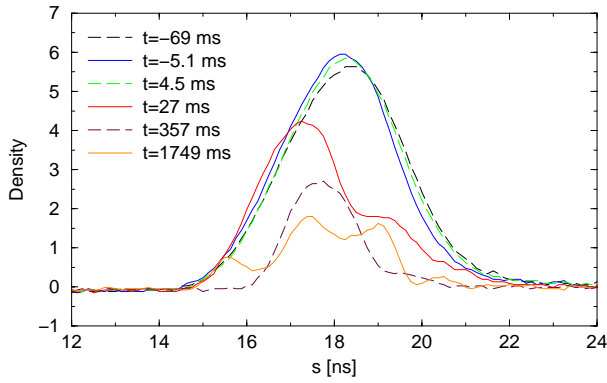


Figure 9: Evolution of the longitudinal profile upon the beam loss near  $\gamma_T$  with  $V_{rf}=300$  kV and  $b_{oct} = -4$  unit.

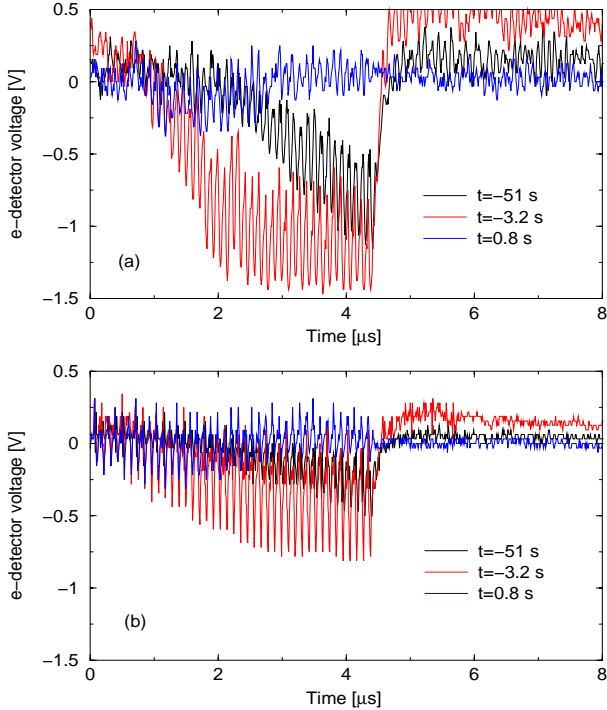


Figure 10:  $e$ -flux measured in the (a) horizontal and (b) vertical directions near  $\gamma_T$ . An ac-coupled amplifier is used with a low-frequency cut-off of about 300 kHz. The grid is not biased. The collector is biased at 50 - 100 V positive.

as the beam approaches  $\gamma_T$ . Associated is the pressure rise both in the warm and cold regions of the ring (Fig. 11).

## DISCUSSIONS AND SUMMARY

Electron cloud is found to be a serious obstacle on the RHIC upgrade path. At merely twice the design number of bunches, electron cloud and electron-ion interactions cause transverse instabilities and emittance growth, and beam loss, along with vacuum pressure rise and background increase. The effect is extremely strong at transition despite the use of  $\gamma_T$ -jump and octupole damping methods.

$e$ -cloud effects occur both in the warm ( $\sim 30\%$  length) and cold ( $\sim 70\%$  length) regions. Nonevaporable-getter (NEG) coating and solenoid windings have been shown to effectively alleviate the effects in the warm section. A

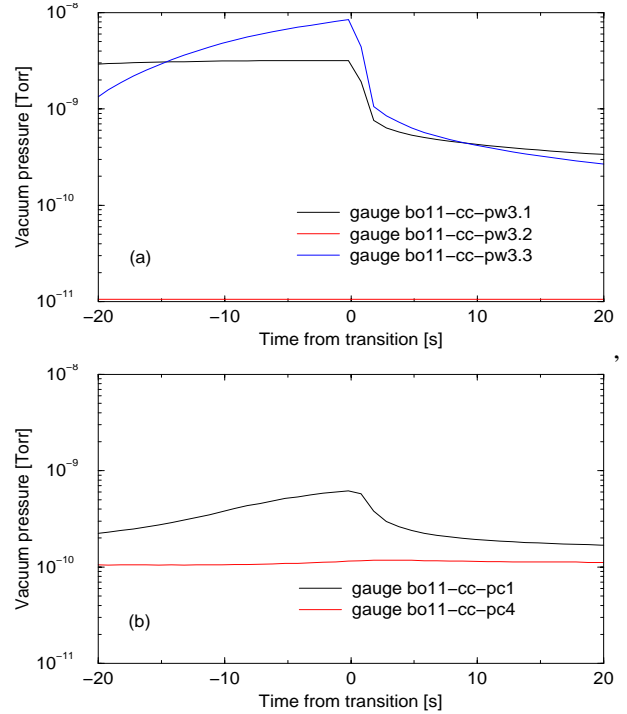


Figure 11: Vacuum pressure rise in the (a) warm and (b) cold region of the ring. Pressure on gauge bo11-cc-pw3.2 located between the two NEG-coated pipes does not rise.

focusing-free transition with reduced peak intensity can possibly mitigate the problem [7].

Many questions remain to be answered. (1) It is not clear why even the first bunch in the train suffers a beam loss much higher than the nominal. One possibility is the multipacting-related gas scattering. More detailed logging of the vacuum pressure (every 0.1 s instead of 1 s) may clarify the mechanism. (2) It is not clear whether the instability alone causes more than 70% beam loss in 0.1 s; what are the principle instability modes [8]; and why beam loss and the transverse instability occur only after but not before transition. A possible explanation yet to be verified is a sizable tune shift due to  $e$ -cloud coupled with a transition-jump lattice close to resonance.  $e$ -detector data needs to be logged in finer steps (1 ns instead of 10 ns) to explore  $e$ -cloud generation within each single bunch.

We thank R. Calaga, H. Hseuh, C. Montag, K. Ohmi, and F. Zimmermann for many helps and discussions.

## REFERENCES

- [1] W. Fischer, M. Blaskiewicz, J.M. Brennan, T. Satogata, Phys. Rev. ST-AB, **5** (2002) 124401
- [2] U. Iriso, et al, BNL Tech. note C-A/AP/129 (2003); ICFA BD News., **33** (2004) 128; BNL Tech. note C-A/AP/191 (2005)
- [3] S.Y. Zhang, BNL Tech. note C-A/AP/67 (2001); S.Y. Zhang, J. Alessi, M. Bai, et al, EPAC'04 (2004) 944
- [4] J. Wei, M. Blaskiewicz, et al, CARE-HHH-APD Workshop, CERN (2004); J. Wei, Rev. Mod. Phys. **75** (2003) 1383
- [5] J. Wei, Ph. D Thesis (1990, Stony Brook)
- [6] C. Montag et al, PRST-AB **7** (2004) 011001; **5** (2002) 084401
- [7] K. Takayama, J. Wei, et al, these proceedings
- [8] M. Blaskiewicz et al, PAC'03 (2003) 3028